Journal of the Virtual Explorer, 2004
Volume 14
Paper 1
http://virtualexplorer.com.au/

Structural mapping of the Eagle Crater outcrop on Mars: New Challenges for the Extraterrestrial Field Geologist

Declan G. De Paor

Department of Earth Sciences, Boston University. Boston, Massachusetts 02215, USA. *Email: ddepaor@bu.edu* .

B. M. Brenton

Department of Earth Sciences, Boston University. Boston, Massachusetts 02215, USA

K. F. Cox

Department of Earth Sciences, Boston University. Boston, Massachusetts 02215, USA

S. R. Duplantis

Department of Earth Sciences, Boston University. Boston, Massachusetts 02215, USA

P. T. Egan

Department of Earth Sciences, Boston University. Boston, Massachusetts 02215, USA

D. E. Kowalewski

Department of Earth Sciences, Boston University. Boston, Massachusetts 02215, USA

P. J. Lancaster

Department of Earth Sciences, Boston University. Boston, Massachusetts 02215, USA

C. A. Masaric-Johnson

Department of Earth Sciences, Boston University. Boston, Massachusetts 02215, USA

H. Melanson

Department of Earth Sciences, Boston University. Boston, Massachusetts 02215, USA

A. J. Orlando

Department of Earth Sciences, Boston University. Boston, Massachusetts 02215, USA

L. M. Sauer

Department of Earth Sciences, Boston University. Boston, Massachusetts 02215, USA

C. M. Witkowski

Department of Earth Sciences, Boston University. Boston, Massachusetts 02215, USA

Keywords: Eagle Crater, Mars, structural geology, fracture cleavage, cross bedding, folding, impact crater

Abstract: We report the results of a structural analysis of the outcrop at Eagle Crater, Meridiani Planum, Mars, which was carried out as an undergraduate class project at Boston University. The outcrop exposes an approximately 20-meter-diameter, semi-circular section of the crater rim in the prevailing down-wind direction. Sedimentary units dip radially outwards on the whole, consistent with an impact origin, though there is some evidence of local folding. Many rock slabs are only slightly out of place, forming a quasi-broken formation that accounts for a sizable portion of the exposure. Geometric features in and around the crater include inclined bedding, cross bedding, undeformed "blueberry" concretions, fracture cleavage, faults, fractures, undeformed crystal vugs, and striations. Observed structures are consistent with an origin by impact cratering and/or wrinkle ridge tectonics. Oblique panorama imagery presented unusual challenges which we overcame with new analytical techniques. Our approach may prove useful for professors and students aiming to understand new forms of field data using the classical techniques of structural analysis.

Table of Contents

Introduction

Background

Boston University's course ES301 - Structural Analysis - was just getting under way in the Spring of 2004 when NASA announced the discovery of an outcrop on Mars, at a location now called Eagle Crater. We had already planned field excursions in Massachusetts and Rhode Island but when the first Martian outcrop was displayed on the NASA Web Site (Figure 1), the addition of a "virtual" field trip to Mars became irresistible.

Using NASA's Maestro program available from http://mars.telascience.org/, in conjunction with data from http://marsrover.nasa.gov/, http://athena.cornell.edu/, and http://marsquestonline.org/, we were able to access and analyze raw images as soon as they were downloaded from the Opportunity rover. Several standard laboratory exercises and class projects were replaced by equivalent exercises using Martian data and the class morphed into an undergraduate research opportunity. Regional SettingMeridiani Planum (a.k.a. Terra Meridiani) is named for its location close to the zero-th meridian on Mars. The Eagle Crater's longitude and latitude (approximately 354° east and 2° south) places it in “a 200 to 300m section of layered rocks that are draped disconformably onto the dissected Noachian cratered terrain” [Arvidson et al. 2003]. These rocks are now thought to be water-lain sediments [Grotzinger 2004, Squyres, S.W. & Athena Team 2004, Squyres & Grotzinger 2004]. A preliminary description of the local geology and geomorphology is given in Arvidson & Athena (2004). We here concentrate on structural analysis of outcrop-scale features.

Figure 1. Panorama of Martian outcrop

Panorama of Martian outcrop taken by Mars Exploration Rover Opportunity on Jan. 27, 2004, while it was still on its landing pad.

NASA Ref: http://photojournal.jpl.nasa.gov/catalog/PIA05158

Structural Mapping on Earth and Mars

Earth-bound structural geologists rely heavily on compass-clinometers to determine the spatial orientations of structures independent of their geographic locations. It is often more important to know that a fracture runs, say, north-south, than to know its precise location to the map to the nearest meter. Statistical analysis of such fracture orientations can yield useful information about the causal stress field, for example. Compass readings are easily corrected for the current declination of Earth's magnetic north pole to yield the direction of true north, and inclinations are estimated using a plumb-line or spirit-level. Unfortunately, these well-established techniques are not transferable to the Martian setting.

Azimuths of Camera Sight-lines

Working with data from the Opportunity rover at Eagle Crater, the first challenge was to determine the azimuths of sight-lines for photographic panoramas relative to the local Martian meridian. The current magnetic field on Mars is exceedingly weak so a compass was not on Opportunity's payload. The above-cited Web Sites displayed frequently updated photographs of the rover's sundial, however the dial changed direction as the rover moved and could not be used for independent determination of azimuth. We thus had to rely on north estimates marked on NASA's map view images or inferred from the edge directions of such images, as determined by mission engineers with access to Opportunity's guidance systems.

Our project base map (Figure 2a) was generated at NASA by distorting panorama photographs and "draping" them on a highly magnified aerial view of the crater taken from orbit. The crater rim is approximately 20m in diameter. The edges of the map view became our standard reference frame Figure 2b and we determined the angular range of panorama photographs by landmark recognition in conjunction with personal communications from Ray Arvidson and other mission scientists. The azimuths of the left and right edges of the panorama in Figure 1 , for example, are 311° and 46° east of north, respectively, and the image spans approximately 12.5° from top to bottom. Given the distortion inherent in stitching photographic panoramas together from multiple images, these determinations are accurate only to within a couple of degrees.

Figure 2a. Outcrop distribution model

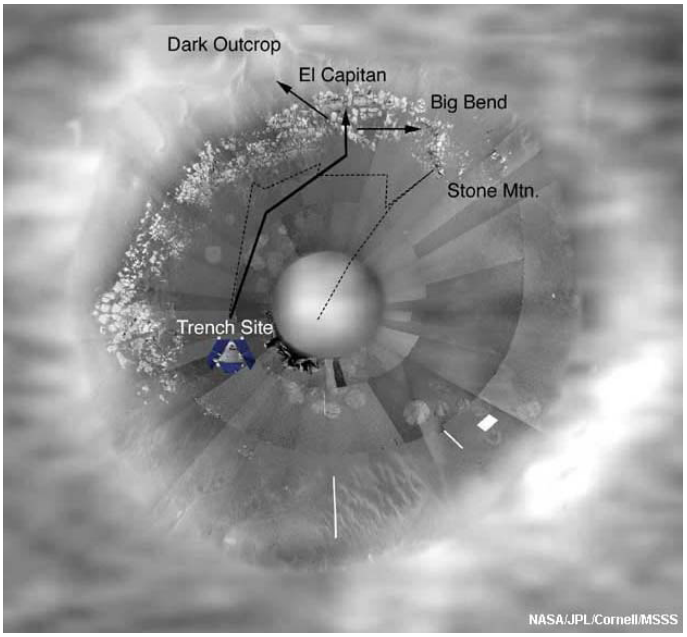

NASA's outcrop distribution model, based on a combination of rover and orbiter data, served as our base map. Locality names and rover tracks are superimposed.

Figure 2b. Mapping Eagle Crater

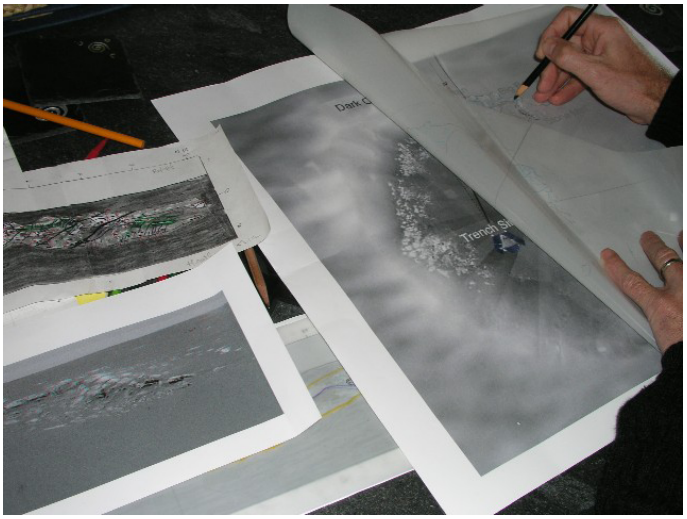

Mapping Eagle Crater.

Inclination Determination

The outcrop panorama was taken while Opportunity was still on its 0.5 meter-high lander (Figure 3a). The camera was mounted on a mast 1.4 meters above the lander pad [Bell et al. 2004], thus 1.9 meters above the ground, and the distance to the outcrop was about 8.0 meters. NASA estimated that the outcrop had a vertical relief of about 0.4 meters. Assuming that the lander rested on approximately level ground, we concluded that the camera's view of the outcrop must have been inclined between 10° and 15° down from the local horizontal. Later, post-egress panoramas were shot from multiple camera viewpoints and stitched together (Figure 3b). These were all approximately 4.0 meters from the crater rim but the camera was 0.5 meters closer to the ground so the inclination angles were still close to the 10° to 15° range.

Figure 3a. Sketch of Opportunity

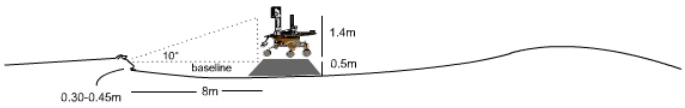

Sketch (not to scale) of Mars Exploration Rover Opportunity resting on its landing pad inside Eagle Crater. Dimensions were used to calculate the camera inclination, as discussed in the text.

Figure 3b. Location key

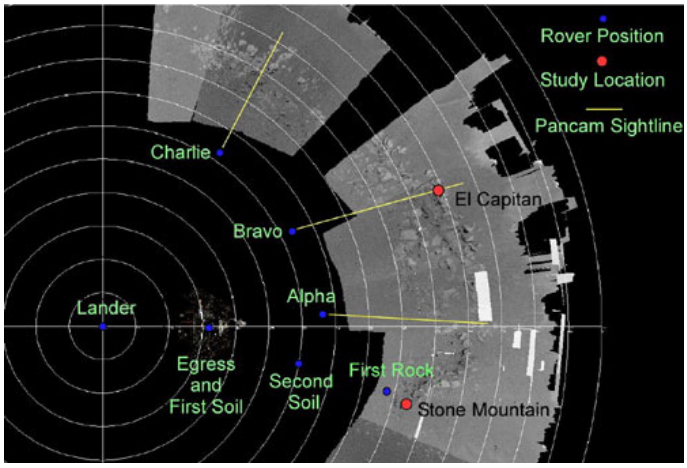

Key to rover locations and Pancam sightlines for detailed studies of the rim outcrop. The circles are spaced 1 meter apart.

Panorama Projection

Rotating a panorama camera's inclined sight-line about a vertical mast results in the generation of a conic surface which can be represented on a standard structural geologists' stereographic projection (Figure 4a , b). By noting sight-line azimuths and inclinations on the panorama, we were able to transfer oblique orientation data onto the stereographic net. However, it was not possible to measure the strike and dip of planar fractures or other planar structures directly from the photographs. Instead, we measured the angle of lean of a fracture's photographic trace relative to

the vertical. Using a protractor, we plotted this data as a short line segment centered on the point in the stereographic projection representing the view direction for that fracture (Figure 4b).

Figure 4. Panorama photo and perspective view

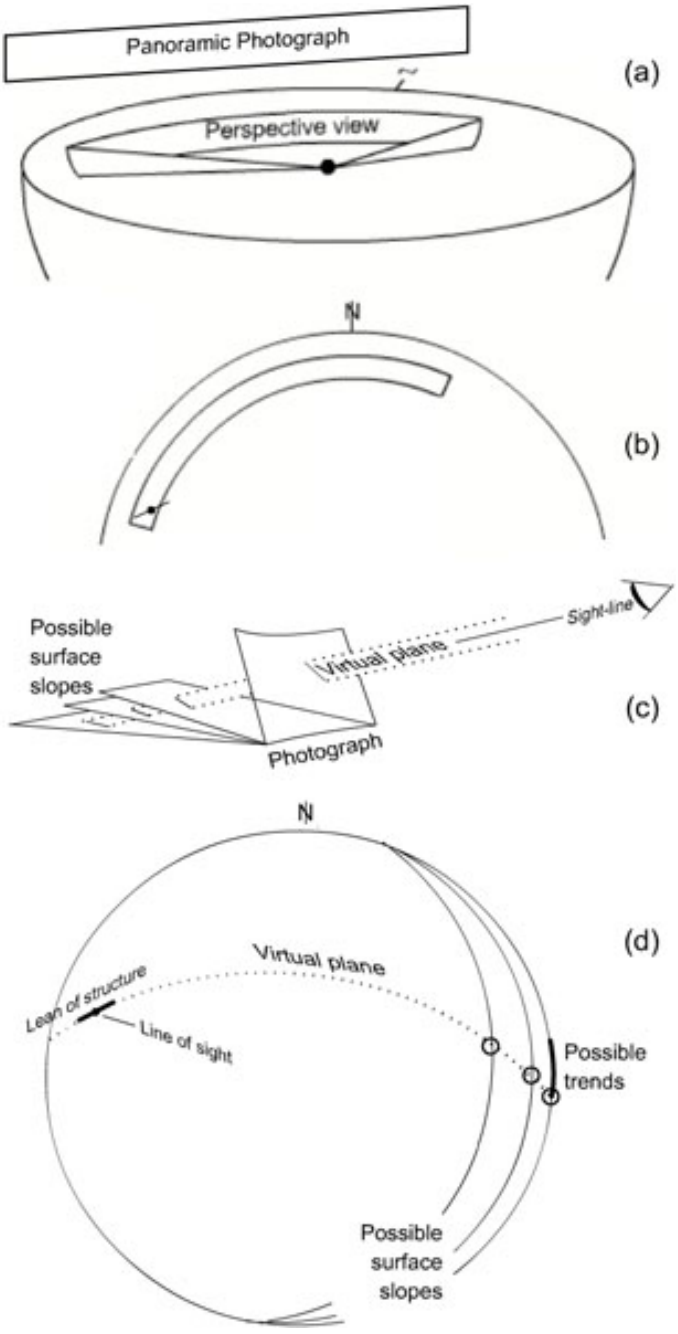

a. Panorama photo and perspective view of the conical surface swept out when an inclined camera pans. N denotes north. Small tick at left of photograph represents the trace of a plane structure such as a fracture on the photograph.

b. Lower hemi- spheric stereographic projection of the panorama. Thanks to the equal-angle property of the projection, lean may be transferred from the photograph to the stereogram using a protractor.

c. The virtual plane defined by the photographic trace and sight-line (perpendicular to the plane of the photo- graph) is here extended to intersect three possible surface slopes.

d. Stereographic projection of the geometry in (c) yields a range of possible structural trends on the ground.Panorama photo and perspective view of the conical surface swept out when an inclined camera pans. N denotes north. Small tick at left of photograph represents the trace of a plane structure such as a fracture on the photograph.

The photographic image of a planar structure only partially constrains the structure's dip. However, on a gently sloping surface, the trace is close to the plane's strike and it is useful to plot this information for a population of structures on a rose diagram, a polar plot of frequency versus azimuth. We therefore devised the following procedure to project the photograph trace back onto the map: The virtual plane defined by the photographic trace plus the camera's line of sight contains lines in a range of orientations, any one of which may be the feature's real surface trace (Figure 4c).

By plotting a great circle to represent this virtual plane, we found its intersections with a set of great circles representing possible surface slopes (Figure 4d). The unique direction that represents the structure's map trace depends on knowledge of the outcrop surface. To narrow the range of possible structural trends we studied anaglyphs of the outcrop with red/blue glasses and qualitatively categorized the 3D surface slopes as gentle, medium, and steep (We experimented with quantitative red/blue parallax measurement, but found that the human eye was adequate for our broad-brush divisions). Inherent in our method of projection data from photographs to the map is the assumption that the surface slopes towards the camera, anti-parallel to the sight-line. This is reasonable, given the rover's location close to the center of the crater, except for the area known as Big Bend. In this area, where the slope is oblique to the camera, surface morphology and coordinate triangulation were used to qualitatively constrain structural trends. For triangulation, we identified three landmarks on a photograph and then determined ternary coordinates of each end of a structural feature in one-to-one correspondence with equivalent map locations (Figure 5). As with petrologic ternary diagrams, only two of the three coordinates are independent variables.

Figure 5. Transfer of structural details

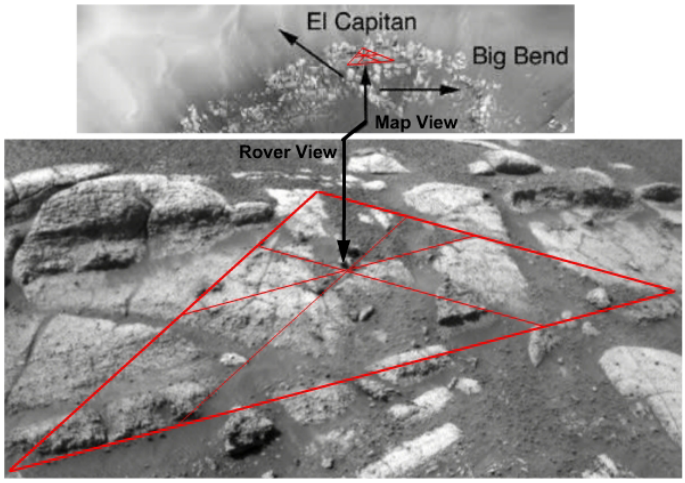

Transfer of structural details from photograph to base map using one-to-one mapping of ternary coordinates. The outcrop relief about 30-40 cm high.

Sometimes, it is useful to estimate the lengths of linear features such as fracture traces in addition to their surface trends. This is accomplished mathematically. If L is the length of a photographic trace oriented at a lean angle of ψ relative to the photograph's vertical edge, Φ is the angle of inclination of the sight-line, and δ is the dip of the surface, which is sloping directly towards the camera, then the length L' of the trace projected onto the surface is:

$$L' = \sqrt{\left(\frac{L \cos\psi}{\sin(\Phi+\delta)}\right)^2 + \left(\frac{L \sin\psi}{1}\right)^2}$$

Virtual Field Observations

Our common Earth-bound field experience leads us to visualize a straight exposure bounded by major fractures or road cuts. In contrast, Opportunity's panoramas of Eagle Crater are tightly wrapped on an approximate 10m radius. The distinction is particularly important for qualitative viewing of the outcrop. For example, parallel fractures are common in terrestrial outcrops and are often attributable to a locally rectilinear stress field. On Martian panoramas, apparently parallel fractures trending away from the viewer correspond to radial fractures on the ground. Such patterns would be highly significant in the tectonic setting of an impact crater. The rover's front and rear hazard cameras ("hazcams") present extremely wide-angle, near fish-eye views. Caution must be exercised in interpreting structures from these sources.

Earth-bound field experience also blinds us to the commonplace. For example, we learn to treat as a nuisance, or at least to ignore, the effects of weathering and erosion on surface exposures. On Mars, evidence for aeolian versus fluvial erosion is of great interest. We had to learn to pay attention to details of outcrop morphology in addition to internal structure.

Structural analysis of Martian bedrock

Exposure

Sands obscure the bedrock in the southeast half of the crater, where higher elevations suggest thick unconsolidated deposits. The greatest outcrop relief, around El Capitan and Big Bend is less than a half meter. Faceted rock surface morphology is typical of exposure by wind abrasion. There are minor gullies that might have been eroded by water but the alternative of wind erosion could not be ruled out (D. Marchant, pers. comm.) and there are no large channels entering or exiting the crater. We conclude that aeolian degradation of the crater rim was the probable cause in exposing bedrock in the northwestern quadrant of Eagle Crater (Figure 2a).

The morphology of Martian craters is dominated by local wind kinematics [Kuzmin et al. 2001, Toigo, A.D. & Richardson, M.I. 2003]. A unidirectional wind pattern heavily degrades the downwind rim of the crater while preserving most of the upwind rim morphology. Where two orthogonal wind directions dominate, an extensive expanse of crater rim is degraded. Atmospheric models predict a directional change of prevailing easterly winds in the Terra Meridiani region due to seasonal effects [Greeley & Thompson 2004]. Extensive and widespread erosion of the Eagle Crater rim is thus consistent with multiple wind directions, mostly from the southeast. Lesser secondary winds may be evidenced by the presence of transverse dunes observed outside the crater.

Bedding

There is evidence for right-way up bedding in the form of cross laminations as previously widely reported [Grotzinger 2004]. Small loose blocks may be inverted but there is no evidence of meso-scale overturning in outcrop. Rose diagrams of bedding traces are dominated by east-west trends consistent with the limits of rim outcrop (Figure 6a).

Big Bend, at the east end of the outcrop, appears to be kink- folded about an oblique axial plane (Figure 6b). The

hinge region is not clearly visible and there may be a concealed fault in the corner of Big Bend. This may represent a minor perturbation of the impact stress field or it may mark a history of deformation involving more than just a single impact event. Judging by homoclinally dipping strata seen at Anatolia, well away from the crater rim, the tilting of sedimentary strata may be a regional phenomenon (Figure 7a), possibly marking the hanging wall of a thrust sheet involved in wrinkle ridge tectonics [Golombek et al 1991, 2001; Okubo & Schultz 2004].

Figure 6a. Rose Diagram of fracture trends

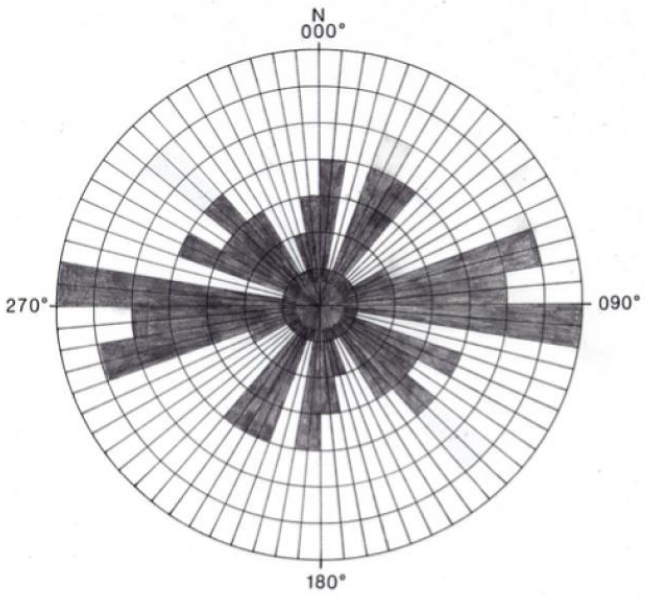

Rose Diagram of fracture trends. n=56. The main cluster is parallel to bedding. Two minor clusters are oblique to bedding.

Figure 6b. Kink folding of beds in the Big Bend

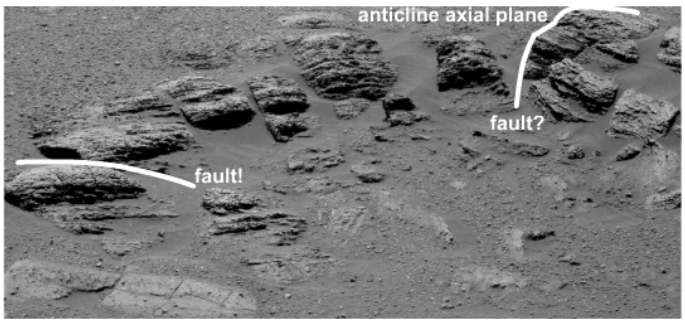

Kink folding of beds in the Big Bend. The core of the fold is poorly exposed and may be faulted. A strike slip fault or slump with pivotal motion is evident at the center left. True thickness of strata is less than 0.5 meter.

Figure 7a. Anatolia

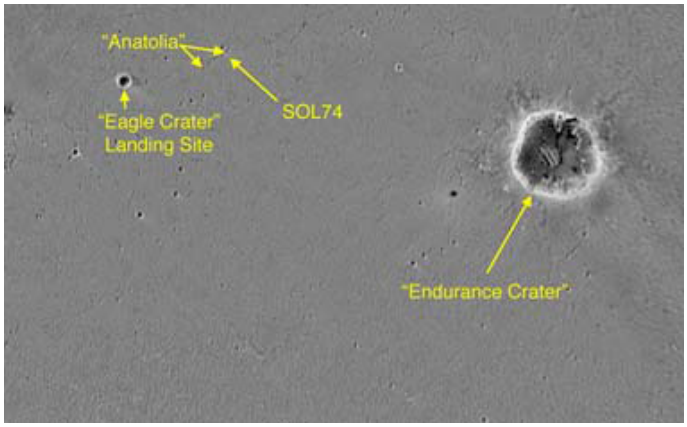

NASA location map for the surface depression called Anatolia.

Figure 7b. Anatolia

Homoclinally dipping strata at Anatolia may represent regional deformation. Bedding traces are exposed mainly as strike sections tangential to the crater rim. Outcrop morphology clearly indicates that the layers dip radially away from the crater rim in general, consistent with an origin by impact, rebound, and rim folding.

There are some parts of the western Eagle Crater rim, here called quasi-broken formation, where bedding traces are not readily discernible (Figure 8a). Apparently loose blocks dominate, but they do not form a jagged topography like that at Fram Crater (Figure 8b). Rather, rock surfaces are dominantly planar and the ground is notably even-paved, like a patio made of stonemason's "crazy pavement." (Unfortunately, we found no evidence of weeds between the paving slabs!) Many adjacent slabs can be fitted back together in jig-saw fashion by closing slightly gaping fractures. Bedding is interpreted to be sub-parallel to surface slope in some of these regions, as confirmed by close-up photography. Bedding in the quasi-broken formation is thus rotated relative to bedding in outcrop but minimally disrupted from one slab to the next. These rocks may

represent extreme aeolian erosion [Williams, S. 2004] or an inner rim collapse structure, or may be the crestal exposure of the fold seen in profile at Big Bend.

Figure 8a. Quasi-broken formation

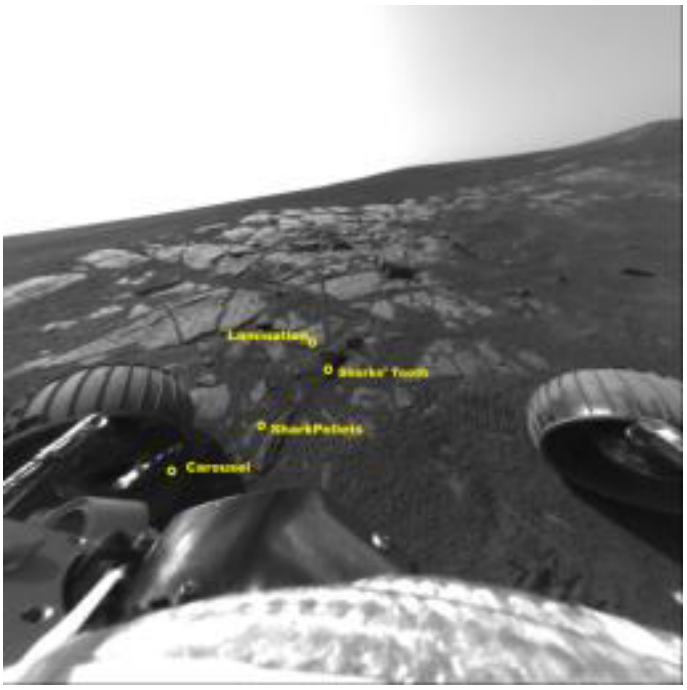

Quasi-broken formation. The ground is remarkably even-paved, like a stone patio. Neighboring slabs fit together in jigsaw fashion.

Figure 8b. Fram Crater

By way of contrast, the rim of Fram Crater is jagged and jumbled.

Faults and Fractures

Many individual sub-meter-scale rocks have inconsistent bedding orientations and are evidently not in place. Since these are clearly the same lithology as the outcrop and occur principally on the inner arc of the rim, they may represent impact-collapse structures. One prominent block at El Capitan has clearly pivoted inwards along a steep oblique fault.

Fracture patterns in the intact outcrop are dominated by relatively short, straight, meter-scale joints and are consistent with an impact origin [Ohman et al. 2003, Rodriguez et al. 2004]. There is no extensive development of conjugate fractures typical of horizontal tectonics on Earth. Fracture frequency in rose diagrams reflects the range of rim outcrop, with significant numbers of NNW orientations.

Fracture patterns in the quasi-broken formation are dominated by triangular slab shapes with many acute dihedral angles (Figure 8a). Small fractures often truncate against the sides of larger triangular slabs in a fractal-like arrangement. Triangular fracture patterns in the quasi-broken formations may be explained by the intersections of radial fractures sets (Figure 8c), by irregular chocolate tablet structure [Figure 4.11A, Ramsay & Huber 1983]. Chocolate tablet structure is possible if elastic rebound from the

impact extended the crater rim in all directions. However, radial fracture sets seem to be the best explanation, given the thin atmosphere and propensity for impact tectonics on the Martian surface. There are also curved fracture patterns that resemble those formed by primary desiccation processes on Earth (Figure 8d , e). Desiccation cracks often have 90 degree joins as well as oblique ones and are generally curved.

Figure 8c. Radiating fracture patterns

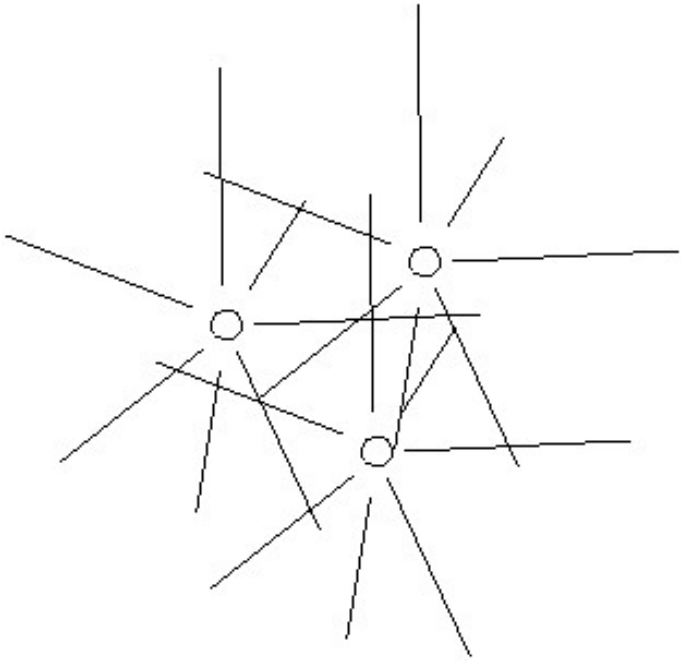

Formation of acute-angled triangular slabs by intersection of radiating fracture patterns.

Figure 8d. Curved joints

Curved joints resembling primary desiccation cracks.

Figure 8e. Desiccation cracks on Earth

Desiccation cracks on Earth Death Valley for comparison, (photo: C. Simpson).

Fracture Cleavage

Several locations exhibit what appears to be a fracture cleavage - a closely spaced penetrative brittle fabric (Figure 9a). Fracture cleavage spacing is similar to the diameters of concentrically zoned spherules ("blueberry"), i.e. 4 to 8 mm on average, and fracture cleavage orientation, where visible, is at a high angle to bedding. Neither bedding nor fracture cleavage appear to wrap around the blueberries. However, some spherical blueberry outlines appear to be cut against cleavage planes, implying a tectonic, post diagenetic origin for the fabric. Some fracture fabrics weather proud, suggesting a possible mineral in-filling; however, photographic resolution is not sufficient to confirm this.

Figure 9a. Fracture cleavage

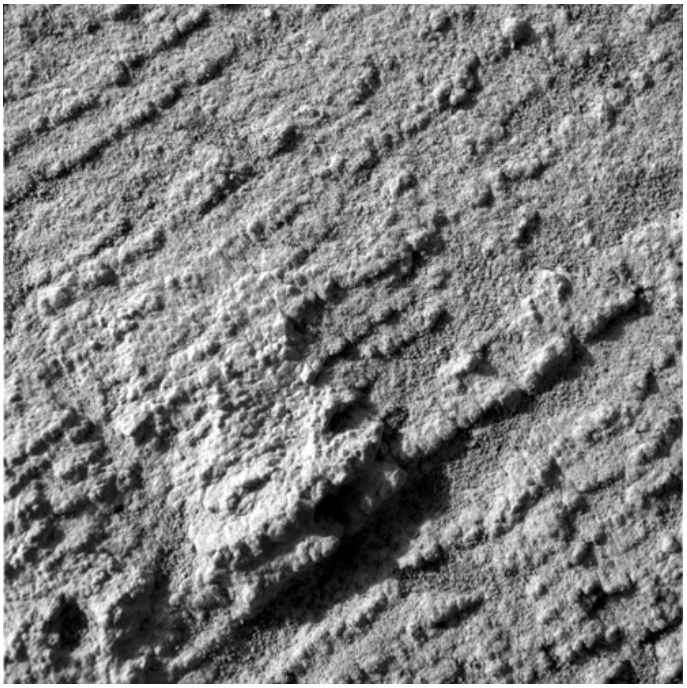

Fracture cleavage at a high angle to bedding

Figure 9b. Crystal vugs

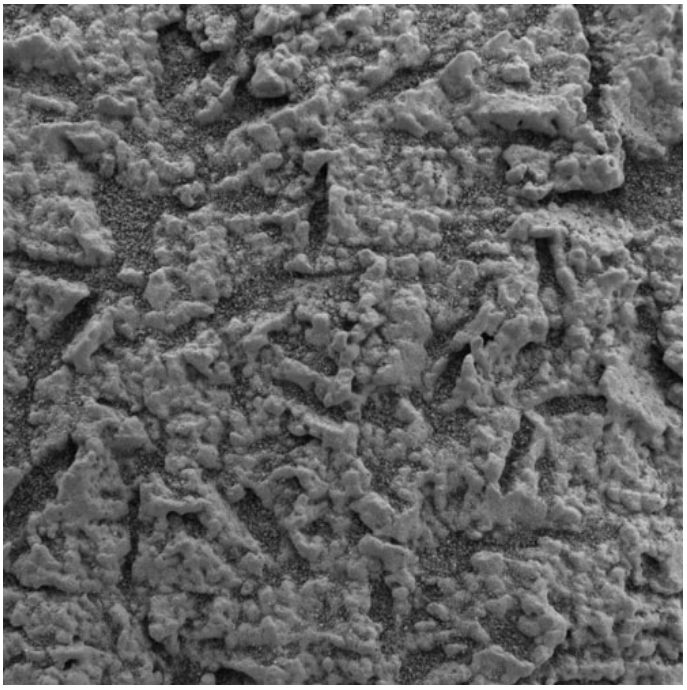

Crystal vugs showing no sign of tectonic strain

Figure 9c. Desiccation cracks on Earth

Striated surface of Bounce Rock.

Crystal Vugs

Study of the orientations of Jarosite crystal casts [Squyres & Grotzinger 2004] reveals no evidence of compaction nor of penetrative finite strain post crystal growth (Figure 9b). Crystals are preferentially aligned at a high angle to bedding but this does not appear to be a strain fabric.

Striations

The surface Bounce Rock, a decimeter-scale loose rock located well outside of the crater rim, has a distinctly striated surface in photographs taken prior to specimen abrasion (Figure 9c). Care is needed in interpreting the specimen because, as its name implies, this rock was hit by the landing module's air bags. However, the striations appear to penetrate the rock and thus could not have been created simply by contact with the air bags. It is possible that the landing impact could have broken open a weak fracture but in that case, the other half of the specimen should be lying nearby on the surface, which it is not. We feel confident that the striations are of pre-mission origin - either due to meteorite impact or tectonic faulting. Striation geometry is consistent with a slickenside of fault origin, which may be mineralized or simply grooved. There are visible steps cross-cutting the striations as commonly described in fault-related slickensides. However, a slight fan-like striation geometry at the edge of the specimen may indicate that it is a shatter cone structure, i.e., a rapidly developed fracture splay formed when the rock was ejected from an impact

site. If the specimen is indeed part of a shatter cone, then it should not differ significantly in composition from the rest of the rock. But if it is a mineralized slickenside, then it may have a very different chemistry to the bulk rock. This issue is significant given the importance attributed to chemical analyses at this location [Mullen 2004, Rayl 2004]. The greasy surface luster supports a meteoritic origin; meteorites commonly acquire a streaky surface sheen as they pass through the atmosphere.

Conclusion

Thanks to the superb educational outreach efforts of NASA and JPL, our virtual class field trip to Eagle Crater on Mars proved highly successful, both as an educational experience and a research opportunity for undergraduates (Figure 10). Several of the structural features that we analyzed have not been previously described by mission scientists. We practiced the classical methods of structural geology using a never-before-seen outcrop, images of which were viewed in near-real time, and this generated much enthusiasm and eagerness. Reliance on mainly oblique panoramic images presented unusual challenges which we overcame with new analytical techniques. Our approach may prove useful for professors and students aiming to understand new forms of extraterrestrial field data using the techniques of classical structural analysis. However, we would emphasize the need for easier access to technical data, such as orientation tick marks on the edges of rover photographs and Euler angles for camera view directions. Given the growth in on-line photographic documentation of outcrops on Earth, our analytical techniques may also prove useful in Earth-bound structural studies.

Figure 10. Analysis lab

Standard structural analysis labs from Boston University course ES301 were adapted to meet the needs of Martian mapping.

Acknowledgments

The first author acknowledges support from the National Science Foundation grant number EAR-0310232. Carol Simpson provided photographs, insights, and stimulating discussion. We thank Ray Arvidson, Jim Head, Sheri Klug, Dave Marchant, Kevin Williams, Maria Zuber, and the NASA JPL outreach staff for taking the time to respond to our numerous email inquiries.

References

Arvidson, R. E., F. P. Seelos, IV, K. S. Deal, W. C. Koeppen. N. O. Snider, J. M. Kieniewicz, B.M. Hynek, M. T. Mellon, and J. B. Garvin, 2003. Mantled and exhumed terrains in Terra Meridiani, Mars, Journal Of Geophysical Research, 108 (E12) 8073.

Arvidson, R.E. and the Athena Science Team, 2004. Geology of Meridiani Planum as inferred from Mars Exploration Rover observations. Lunar and Planetary Science Institute, XXXV, 2165.pdf

Bell III, J.F., S.W. Squyres, R.E. Arvidson, H.M. Arneson, D. Bass, N. Cabrol, W. Calvin, J. Farmer, W.H. Farrand, W. Goetz, M. Golombek, J. Grant, J. Grotzinger, E. Guinness, L. Haskin, A.G. Hayes, K.E. Herkenhoff, M.J. Johnson, J.R. Johnson, J. Joseph, K. Kinch, M.T. Lemmon, M.B. Madsen, J.N. Maki, E. McCartney, S. McLennan, H.Y. McSween, M. Malin, D.W. Ming, R.V. Morris, E.Z. Noe Dobrea1, T.J. Parker, J. Proton, J. Rice, F. Seelos, J. Soderblom, L.A. Soderblom, J.N. Sohl-Dickstein, R.J. Sullivan, M.J. Wolff, A. Wang, and Athena Science Team, 2004. Pancam Imaging of the Mars Exploration Rover Landing Sites in Gusev Crater and Meridiani Planum. Lunar and Planetary Science Institute XXXV, 2169.pdf

Greeley, R. and S.D. Thompson, 2003. Mars: Aeolian features and wind predictions at the Terra Meridiani and Isidis Planitia potential Mars Exploration Rover landing sites, Journal of Geophysical Research, v. 108 (E12), 8093.

Golombek, M.P., J.B. Plescia, and B.J. Franklin, 1991, Faulting and folding in the formation of planetary wrinkle ridges, in Proceedings of the 21st. Lunar and Planetary Science Conference, Houston, Lunar and Planetary Institute, p. 679-693.

Golombek, M.P., F.S. Anderson, and M.T. Zuber, 2001, Martian wrinkle ridge topography — Evidence for subsurface faults from MOLA: Journal of Geophysical Research, v. 106, p. 23,81123,821.

Grotzinger, J. 2004. http://origin.mars5.jpl.nasa.gov/gallery/press/opportunity/20040211a.html

Kuzmin, R.O., R. Greeley, S.C.R. Rafkin, and R.M. Haberle, 2001. Wind related modification of some small impact craters on Mars. Icarus 153: 61-70.

Okubo C.H., & R.A. Schultz, 2004. Mechanical stratigraphy in the western equatorial region of Mars based on thrust faultrelated fold topography and implications for near-surface volatile reservoirs. GSA Bulletin v. 116; no. 5/6; p. 594605.

Ramsay, J.G. & M. Huber, 1983. The Techniques of Modern Structural Geology. Academic Press, N.Y. 307pp.

Rayl, A.J.S. 2004. http://www.planetary.org/news/2004/mer-update_04-04-17.html

Squyres, S.W. & Athena Team 2004. Initial results from the Mer athena science investigation at Gusev crater and Meridiani Planum. Lunar & Planetary Science XXXV 2187.pdf http://www.lpi.usra.edu/meetings/lpsc2004/pdf/2187.pdf

Squyres, S.W. & J. Grotzinger, 2004. http://www.geotimes.org/mar04/WebExtra030204.html

Toigo, A.D. & M.I. Richardson, 2003. Meteorology of proposed Mars Exploration Rover landing sites. Journal of Geophysical Research v. 108 (E12) 8092.

Williams, S. 2004: Winds of Mars: Aeolian Activity and Landscape. http://www.lpi.usra.edu/publications/slidesets/winds/

Error: no bibliography entry: d0e709 found in http://docbook.sourceforge.net/release/bibliography/bibliography.xml